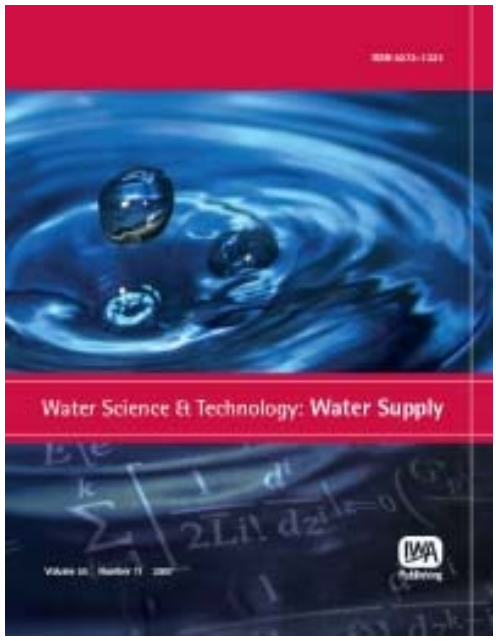

Accurate water hammer pressure modeling for automatic modification of stress distribution along multi-segment pipelines

A. Abbasi, S. R. Sabbagh-Yazdi and F. M. Wegian

ABSTRACT

In this study, automatic modification of stresses in rigid parts of a pipe line system is modeled using the trial results of a second-order explicit Finite Volume (FV) Godunov type scheme for one-dimensional transient flow in pipes. The developed model for numerical analysis of transient pressure is based on Riemann solution of continuity equation coupled with the momentum Equation (including convective term). The implementation of boundary conditions such as reservoirs, valves, and pipe junctions in the Godunov approach is similar to that of the method of characteristics (MOC) approach. The computed pressure waves are compared with analytical solution as well as laboratory measurements for single pipes. The model is applied on two classic problems (systems consisting of a reservoir, a pipe and a valve). The second-order Godunov scheme is stable for Courant number less than or equal to unity, and therefore, can be applied for the problems with variable mesh spacing. In order to show the ability of the developed model to deal with such cases, the computed maximum pressure distribution along a pipeline with variable segment coordinates are used for trial modification of pipe thickness and stress distribution.

Key words | convective term, finite volume method, Riemann problem, stress distribution, water hammer

A. Abbasi
S. R. Sabbagh-Yazdi
Civil Engineering Department,
K.N. Toosi University of Technology,
PO Box 1346, Valiasr Street,
Tehran,
Iran
E-mail: *AliAbbasi.civileng@gmail.com*; *SYazdi@kntu.ac.ir*

F. M. Wegian (corresponding author)
Civil Engineering Department,
College of Technological Studies (Kuwait),
The Public Authority for Applied Education and Training,
PO Box 27590,
Safat 13136 Shuwaikh,
Kuwait
E-mail: *fmwm@yahoo.com*

INTRODUCTION

Transient flow caused by pump shutdowns, or rapid changes in valve setting, trigger a series of positive and negative pressure waves large enough to rupture pipelines or damage other hydraulic devices. Positive pressures may end up with over stressing in rigid parts and consequent damages to the pipe line system. Negative pressure waves can also result in cavitations, pitting and corrosion. Thus, accurate modeling of water hammer problems in pipes is vital for proper design and safe operation of pressurized pipeline systems. Therefore, the design of pipeline systems requires efficient mathematical models capable of accurately solving water hammer problems.

Various numerical approaches have been introduced for pipeline transient flow calculation. They include the Method of Characteristics (MOC) (Ghidaoui & Karney 1994), Finite Difference (Chaudhary & Housaini 1985), Finite Element (FE) (Jovic 1995), and Finite Volume (FV).

Among these methods, MOC proved to be the most popular among water hammer experts. However, in order to improve the shortcomings of the MOC, some numerical workers tried to combine MOC with other solution methods (Afshar & Rohani 2008).

The MOC approach transforms the water hammer partial differential equations into ordinary differential equations along characteristic lines. The integration of these ordinary differential equations from one time step to the next requires that the value of the head and flow at the foot of each characteristic line be known. This problem can be overcome by one of the following approaches: (i) using the MOC-grid scheme; or (ii) using the fixed-grid MOC

doi: 10.2166/ws.2009.362

scheme and employ interpolation in pipe direction. For the later approach, it is impossible to make the Courant number exactly equal to one in all pipes. Therefore, unwanted numerical damping and accuracy degradation may associate with application of MOC, when the Courant number is less than one (Afshar & Rohani 2008).

Although the implicit FD methods do not have the Courant number restriction, they suffer from heavy computational work loads and large storage requirements. Most of the implicit solvers not only necessitate a dedicated matrix inverse solvers but also iterative schemes for their solution procedures. The most important problem with the implicit method is distortion of the physical path of wave propagations and their region of influence and domain of dependence. Although the results of solving the water hammer equations by explicit FD schemes, show that these second-order FD schemes produce better results than the first-order MOC, the restriction of choice of Courant number and requirement for equally spaced grid points are some of the short coming of this method (Chaudhary & Housaini 1985).

FE methods are known for their ability to: (i) use unstructured grids (meshes), (ii) provide fast convergence and accurate results, and (iii) provide results in any point of problem domain (Jovic 1995). However, the computational work load of the FE solvers motivates the research works on improvement of numerical solvers. For instance, Jovic (1995) used the combined method of MOC and FE for water hammer modeling in a classical system (a system consisting of a reservoir, a pipe, and a valve).

FV methods are widely used in the solutions of hyperbolic systems, such as gas dynamics and shallow water waves. FV methods are noted for their ability to: (i) conserve mass and momentum, (ii) provide sharp resolution of discontinuities without spurious oscillations, and (iii) use unstructured grid (mesh). The first order FV method for solution of water hammer problems was highly similar to MOC with linear space-line interpolation (Zhao & Ghidaoui 2004). Application of Godunov scheme for the second order FV solution of continuity and momentum equations without convective term produced accurate results for very low Mach numbers (Zhao & Ghidaoui 2004). Using transient friction in second order FV method has improved the accuracy of the results (Abbasi & Sabbagh-Yazdi 2009).

In this article, the Godunov type for FV solution of transient continuity equation coupled with momentum equation without dropping the convective term (which is not essential for the cases in which the Mach number is not very low) is applied for numerical analysis of transient pressure. After investigation of the accuracy of the model for computation of transient pressure in a pipe, the model is developed for automatic modification of stress distribution along a multi segments pipeline. The paper is organized as follows. First, the governing equations of water hammer are given. Second, the FV form of the governing equations is provided, and then, second-order Godunov scheme for the FV fluxes are formulated, and, the time integration of the equations is derived. Third, internal and boundary conditions for solution of the transient flow problem in pipes are reviewed. Fourth, the schemes are tested using single pipe systems. Finally, the developed model is verified for the pipes without and with wall frictions, and then, it is applied for a real world problem of multi segments pipeline.

GOVERNING EQUATIONS

In the absence of column separation, transient flow in a closed conduit is often mathematically described by a set of one-dimensional hyperbolic partial differential equations including the section averaged incompressible continuity and momentum (Balino *et al.* 2001):

$$\frac{\partial H}{\partial t} + V\frac{\partial H}{\partial x} + \frac{a^2}{g}\frac{\partial V}{\partial x} = -V\sin\theta \tag{1}$$

$$\frac{\partial V}{\partial t} + V\frac{\partial V}{\partial x} + g\frac{\partial H}{\partial x} = -J \tag{2}$$

$$H = \frac{P}{\rho g} + Z \tag{3}$$

In above equations, t: time; x: distance along the pipe centerline; $H = H(x,t)$: piezometric head; $V = V(x,t)$: instantaneous average fluid velocity; g: gravitational acceleration; θ: the pipe slope; P: pressure; ρ: fluid density and Z: level. In the continuity equation, the wave speed, a, is defined as (Balino *et al.* 2001),

$$a = \left[\frac{(K/\rho)}{(1 + KD/Ee)}\right]^{1/2} \tag{4}$$

Here, K: bulk modulus of elasticity of the fluid; E: Young's modulus of elasticity for the pipe; ρ: density of the fluid; and e: thickness of the pipe.

In the momentum equation, J is the global friction force due to the wall friction is modeled using the following formula (Pezzinga 2000):

$$J = \frac{fV|V|}{2D} + k\left(\frac{\partial V}{\partial t}\right) - k\left(a\frac{\partial V}{\partial x}\right) \tag{5}$$

where, D is pipe diameter; f is Darcy-Weisbach friction factor, and k: unsteady friction factor. The nonlinear convective terms $V\partial H/\partial x$ and $V\partial V/\partial x$ are included in Equations (1) and (2). These terms, although small for the majority of water hammer problems, are not neglected in this paper. Maintaining the convective terms in the governing equations makes the scheme applicable to a wide range of transient flow problems.

FINITE VOLUME FORMULATION

The numerical modeling of the computational domain involves the discretization of the x axis into reaches, each of which has a length Δx and the t axis into intervals each of which has duration Δt. Node (i,n) denotes the point with coordinate $x = [i - (1/2)]\Delta x$ and $t = n\Delta t$. A quantity with a subscript i and a superscript n signifies that this quantity is evaluated at node (i,n) (Figure 1).

The control volume i is centered at node i and extends from $(i - 1/2)$ to $(i + 1/2)$. That is, the ith control volume is defined by the interval $[(i - 1)\Delta x,\ i\Delta x]$. The boundary between control volume i and control volume $(i + 1)$ has a coordinate $(i{\cdot}\Delta x)$ and is referred to either as a control surface or a cell interface. Quantities at a cell interface are identified by subscript such as $(i - 1/2)$ and $(i + 1/2)$ (Figure 2).

Based on the Riemann solution, the FV discretization of Equations (1) and (2) in the ith control volume entails the

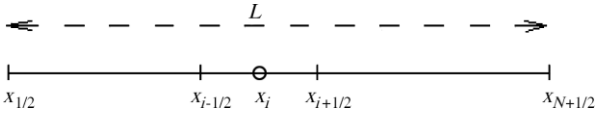

Figure 1 | Discretization of the space domain.

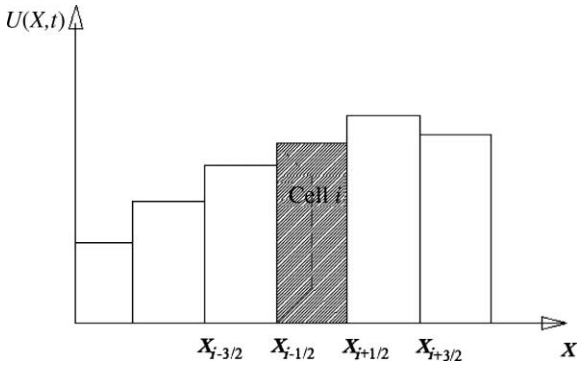

Figure 2 | One-dimensional control volume.

following steps: (a) the governing equations are rewritten in control volume form; (b) the fluxes at a control surface are approximated using the exact solution of the Riemann problems; and (c) a time integration to advance the solution from n to $n + 1$ (Zhao & Ghidaoui 2004).

Equations (1) and (2) can be rewritten in non-conservative form, as (Guinot 2000),

$$\frac{\partial \boldsymbol{u}}{\partial t} + \frac{\partial \boldsymbol{f}(\boldsymbol{u})}{\partial x} = \boldsymbol{s}(\boldsymbol{u}) \tag{6}$$

where $f(\boldsymbol{u}) = \bar{\boldsymbol{A}}\boldsymbol{u}$,

$$\bar{\boldsymbol{A}} = \begin{pmatrix} \bar{V} & a^2/g \\ g & \bar{V} \end{pmatrix}$$

and $\bar{V}$: mean value of V to be specified later. Setting $\bar{V} = 0$, the scheme reverts to the classical water hammer case where the convective terms are neglected.

The continuity and momentum equations for control volume i is obtained by integration Equation (6) with respect to x from control surface $(i - 1/2)$ to control surface $(i + 1/2)$. The results are:

$$\frac{\mathrm{d}}{\mathrm{d}t}\int_{i-1/2}^{i+1/2} \boldsymbol{u}\,\mathrm{d}x + \boldsymbol{f}_{i+1/2} - \boldsymbol{f}_{i-1/2} = \int_{-1/2}^{i+1/2} \boldsymbol{s}\,\mathrm{d}x \tag{7}$$

The above equation is the statement of laws for incompressible form of the continuity and momentum conservation

for the ith control volume. Let U_i = mean value of $\boldsymbol{u}$ in the interval $[i-1/2, i+1/2]$. Equation (7) becomes:

$$\frac{\mathrm{d}\boldsymbol{U}}{\mathrm{d}t} = \frac{\boldsymbol{f}_{i-1/2} - \boldsymbol{f}_{i+1/2}}{\Delta x} + \frac{1}{\Delta x}\int_{i-1/2}^{i+1/2} \boldsymbol{s}\mathrm{d}x \tag{8}$$

Note that, the fluxes at cell interfaces can be determined from the Godunov scheme that requires the exact solution of the Riemann problem. Godunov schemes are conservative, explicit, and efficient. The formulation of a Godunov scheme for the mass and momentum flux $\boldsymbol{f}_{i+1/2}$ in Equation (8) for all i and for $t \in [t^n, t^{n+1}]$ requires the exact solution of the following Riemann problem (Figure 3):

$$\frac{\partial \boldsymbol{u}}{\partial t} + \frac{\partial \boldsymbol{f}(\boldsymbol{u})}{\partial x} = 0 \tag{9}$$

where

$$\boldsymbol{u}^n(x) = \begin{cases} \boldsymbol{U}_L^n & \text{for} \quad x < x_{i+1/2} \\ \boldsymbol{U}_R^n & \text{for} \quad x > x_{i+1/2} \end{cases} \tag{10}$$

$\boldsymbol{U}_L^n$ is the average value of $\boldsymbol{u}$ to the left of interface $(i+1/2)$ at n (it can be guessed from the average values $\boldsymbol{u}$ in the left neighboring cell); and $\boldsymbol{U}_R^n$ is average value of $\boldsymbol{u}$ to the right of interface $(i+1/2)$ at n (it can be guessed from the average values $\boldsymbol{u}$ in the right neighboring cell) (Figure 4).

The exact solution of Equation (9) at $(i+1/2)$ for all internal nodes i and for $t \in [t^n, t^{n+1}]$ is as follows:

$$\boldsymbol{u}_{i+1/2}(t) = \begin{pmatrix} H_{i+1/2} \\ V_{i+1/2} \end{pmatrix} = \frac{1}{2}\begin{pmatrix} (H_L^n + H_R^n) + \frac{a}{g}(V_L^n - V_R^n) \\ (V_L^n + V_R^n) + \frac{g}{a}(H_L^n - H_R^n) \end{pmatrix}$$
$$= \boldsymbol{B}\boldsymbol{U}_L^n + \boldsymbol{C}\boldsymbol{U}_R^n \tag{11}$$

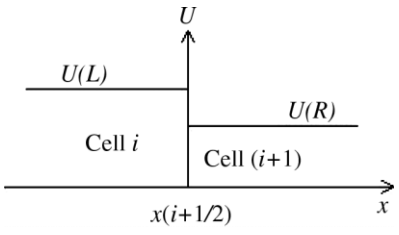

Figure 3 | Definition of a Riemann problem.

Here,

$$\boldsymbol{B} = \frac{1}{2}\begin{pmatrix} 1 & a/g \\ g/a & 1 \end{pmatrix} \quad \text{and} \quad C = \frac{1}{2}\begin{pmatrix} 1 & -a/g \\ -g/a & 1 \end{pmatrix}.$$

The volume and incompressible flow momentum fluxes at $(i+1/2)$ for all internal nodes and for $t \in [t^n, t^{n+1}]$ can be formulated using the above equation, as follow:

$$\boldsymbol{f}_{i+1/2} = \bar{\boldsymbol{A}}_{i+1/2}\boldsymbol{u}_{i+1/2} = \bar{\boldsymbol{A}}_{i+1/2}\boldsymbol{B}\boldsymbol{U}_L^n + \bar{\boldsymbol{A}}_{i+1/2}\boldsymbol{C}\boldsymbol{U}_R^n \tag{12}$$

In order to evaluate the right-hand side of the above equation, $\bar{\boldsymbol{A}}_{i+1/2}$, $\boldsymbol{U}_L^n$, and $\boldsymbol{U}_R^n$ are to be approximated. To estimate $\bar{\boldsymbol{A}}_{i+1/2}$, the entry associated with the advection terms, $\bar{V}_{i+1/2}$, needs to be approximated. Setting $\bar{V} = 0$ is equivalent to neglecting the advection terms from the governing equations. In general, an arithmetic mean is used to evaluate $\bar{V}_{i+1/2}$.

Second-order Godunov scheme

In present work, the second order scheme of Godunov type finite volume is adopted. For such a scheme limiters increase the order of accuracy of a scheme while ensuring that results are free of spurious oscillations.

By application of following stages at every time step, an approximation for $\boldsymbol{U}_L^n$ and $\boldsymbol{U}_R^n$ that is second order in space and time is obtained using MINMOD limiter (Zhao & Ghidaoui 2004):

At the first stage:

$$\boldsymbol{U}_{i-(1/2)^+}^n = \boldsymbol{U}_i^n - 0.5\Delta x \mathrm{MINMOD}(\sigma_j^n, \sigma_{j-1}^n) \tag{13}$$

and

$$\boldsymbol{U}_{i+(1/2)^-}^n = \boldsymbol{U}_i^n + 0.5\Delta x \mathrm{MINMOD}(\sigma_j^n, \sigma_{j-1}^n) \tag{14}$$

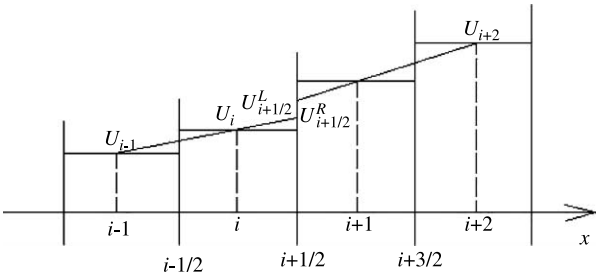

Figure 4 | Sketch of variable at the cell interface.

where,

$$\text{MINMOD}(\sigma_j^n, \sigma_{j-1}^n) = \begin{cases} \min(\sigma_j^n, \sigma_{j-1}^n) & \text{if} \quad \sigma_j^n, \sigma_{j-1}^n \geq 0 \\ \max(\sigma_j^n, \sigma_{j-1}^n) & \text{if} \quad \sigma_j^n, \sigma_{j-1}^n \leq 0 \\ 0 & \text{otherwise} \end{cases} \tag{15}$$

Here,

$$\sigma_{j-1}^n = (\boldsymbol{U}_j^n - \boldsymbol{U}_{j-1}^n)/\Delta x \tag{16}$$

and

$$\sigma_j^n = (\boldsymbol{U}_{j+1}^n - \boldsymbol{U}_j^n)/\Delta x \tag{17}$$

At the second stage:

$$\boldsymbol{U}_{i+(1/2)^-}^{n^*} = \boldsymbol{U}_{i+(1/2)^-}^n + \frac{1}{2}\frac{\Delta t}{\Delta x}\left[\boldsymbol{f}(\boldsymbol{U}_{i-(1/2)^+}^n) - \boldsymbol{f}(\boldsymbol{U}_{i+(1/2)^-}^n)\right] \tag{18}$$

and

$$\boldsymbol{U}_{i-(1/2)^+}^{n^*} = \boldsymbol{U}_{i-(1/2)^+}^n + \frac{1}{2}\frac{\Delta t}{\Delta x}[\boldsymbol{f}(\boldsymbol{U}_{i-(1/2)^+}^n) - \boldsymbol{f}(\boldsymbol{U}_{i+(1/2)^-}^n)] \tag{19}$$

Finally, the second order scheme is approximated as:

$$\boldsymbol{U}_R^n = \boldsymbol{U}_{i+(1/2)^+}^{n^*} \quad \text{and} \quad \boldsymbol{U}_L^n = \boldsymbol{U}_{i+(1/2)^-}^{n^*} \tag{20}$$

Godunov second-order scheme for the solution of Equation (6) can be achieved by inserting Equation (20) into Equation (12).

TIME INTEGRATION

Explicit evaluation of the Equations (11) and (12) can provide light computational work load if time stepping restriction (Courant number limit) is considered proportional to the smallest special interval along the computational domain. However, low order explicit schemes usually suffer from numerical instabilities that may cause serious problems for the solution procedure. Hence, the time stepping of explicit solution of the convective part of the hyperbolic type equations should satisfy the Courant-Friedrichs-Lewy condition ($Cr = a\Delta t/\Delta x \leq 1$).

The explicit evaluation of Equations (11) and (12) requires that $\boldsymbol{U}_L^n$ and $\boldsymbol{U}_R^n$ are properly evaluated in terms of known nodal values at time stage t^n.

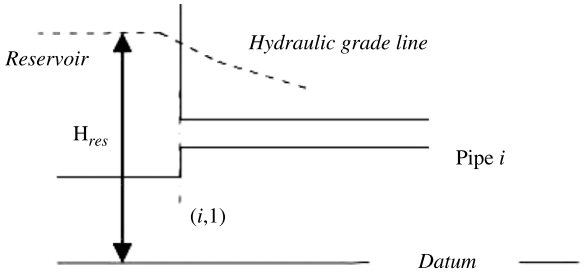

Figure 5 | Constant level upstream reservoir.

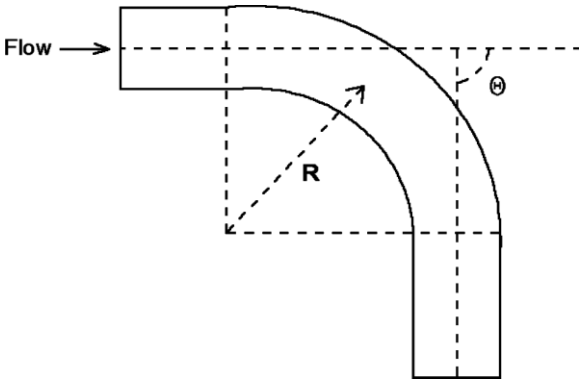

Figure 6 | Bend characteristic parameters.

BOUNDARY AND INTERNAL CONDITIONS

The techniques for imposing of boundary and internal conditions are an important step in a numerical simulation. The boundary and internal conditions in this model are as follow:

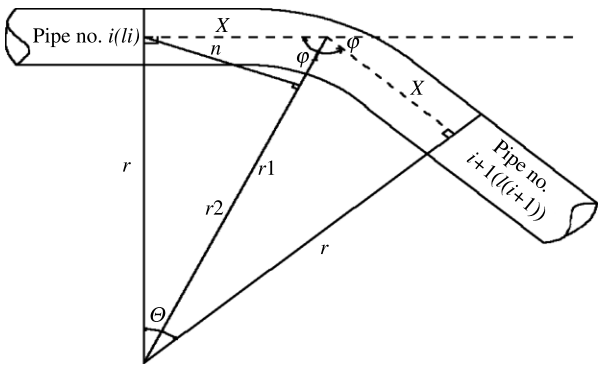

Figure 7 | Bend characteristic parameter in model.

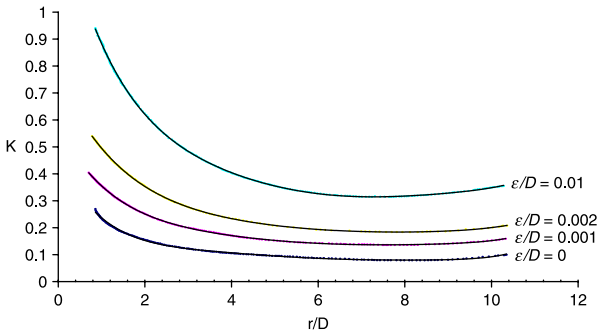

Figure 8 | A sample graph for bend head loss coefficient (associate with angle $\theta = \pi/2$) application of developed model ($\sigma = \rho g H \times D/2t$).

Head-constant upstream reservoir

The flux at an upstream boundary (i.e. $i = 1/2$) can be determined from the Riemann solution. The Riemann invariant associated with the negative characteristic line is:

$$H_{1/2} - \frac{a}{g}V_{1/2} = H_1^n - \frac{a}{g}V_1^n \tag{21}$$

Coupling this Riemann invariant with a head-flow boundary relation determines:

$$V_{1/2}^{n+1} = V_{1\frac{1}{2}}^n + \frac{g}{a}\left(H_{1/2} - H_{1\frac{1}{2}}^n\right) \tag{22}$$

For a constant level upstream reservoir (Figure 5), where $H_{1/2}^n = H_{\text{res}}$, the flux at the upstream boundary is (Zhao & Ghidaoui 2004):

$$\boldsymbol{f}_{1/2} = \begin{bmatrix} \bar{V}_{1/2}H_{\text{res}} + \frac{a^2}{g}(V_1^n + \frac{g}{a}(H_{\text{res}} - H_1^n)) \\ gH_{\text{res}} + \bar{V}_{1/2}(V_1^n + \frac{g}{a}(H_{\text{res}} - H_1^n)) \end{bmatrix} \tag{23}$$

Fully closed downstream valve

The flux at a downstream boundary can be determined from the Riemann solution. The Riemann invariant associated with the positive characteristic line is:

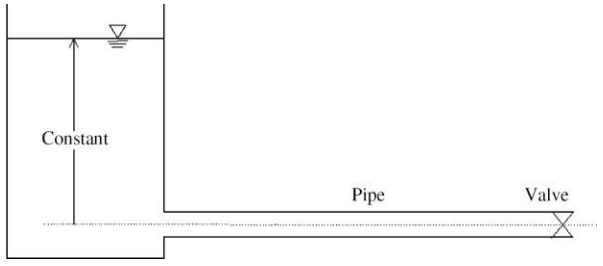

Figure 9 | A simple reservoir-pipe-valve configuration.

Table 1 | Geometrical and hydraulic parameters for test case without friction

Pipe diameter (m)	0.5
Pipe length (m)	1000
DW friction factor	0.00
Unsteady friction factor	0.00
Wave speed (m/s)	1000
Reservoir head-upstream (m)	0
Initial mean velocity (m/s)	1.02
Cause of transients	Downstream instantaneous fully valve closure

$$H_{Nx+1/2} + \frac{a}{g}V_{Nx+1/2} = H_{Nx}^n + \frac{a}{g}V_{Nx}^n \tag{24}$$

Downstream boundary condition is valve closure in T_c. Head-flow boundary relation determines:

$$V_{Nx+1/2}^{n+1} = V_{\text{steady}}(1 - \frac{t}{T_c}) \quad 0 \le t \le T_c \tag{25}$$

$$V_{Nx+1/2}^{n+1} = 0 \quad t > T_c \tag{26}$$

$$H_{Nx+1/2}^n - H_{Nx-1/2}^n - \frac{a}{g}(V_{Nx+1/2}^{n+1} - V_{Nx-1/2}^n) = 0 \tag{27}$$

As a result, the flux at the boundary is determined as follows (Zhao & Ghidaoui 2004):

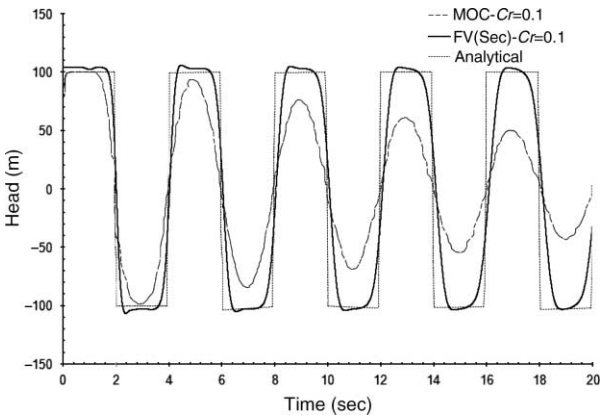

Figure 10 | Variations in hydraulic head at the valve position for a frictionless pipe resulted from MOC and present FV solvers and compared with analytical solution.

Table 2 | Properties for the test case with friction

Pipe diameter (m)	0.022
Pipe length (m)	37.20
DW friction factor	0.034
Unsteady friction factor	0.00
Wave speed (m/s)	1319
Reservoir head-upstream (m)	32.0
Discharge (L/s)	0.114
Density (kg/m^3)	1000
Viscosity (m^2/s)	1.02
Cause of transients	Downstream valve closure in 0.009 seconds

$$\boldsymbol{f}_{Nx+1/2} = \begin{bmatrix} \bar{V}_{Nx+1/2}(H_{Nx} + \frac{a}{g}V^n_{Nx} - \frac{a}{g}V_{Nx+1/2}) + \frac{a}{g}V_{Nx+1/2} \\ g(H_{Nx} + \frac{a}{g}V^n_{Nx} - \frac{a}{g}V_{Nx+1/2}) + \bar{V}_{Nx+1/2}V_{Nx+1/2} \end{bmatrix} \tag{28}$$

Bend effect

The local bends in the pipeline may cause a head loss. Therefore, the following local head loss must be considered in J as the global friction force due to the bend effect at the nodal point associate with the bend location.

$$h_{lb} = K\frac{V_1^2}{2g} \tag{29}$$

The parameter K is the bend head loss coefficient which depends to the bend angle (θ), pipe diameter (D), relative friction (ε/D) and bending length of the pipes which depends to the bend radius r as shown in Figures 6 and 7.

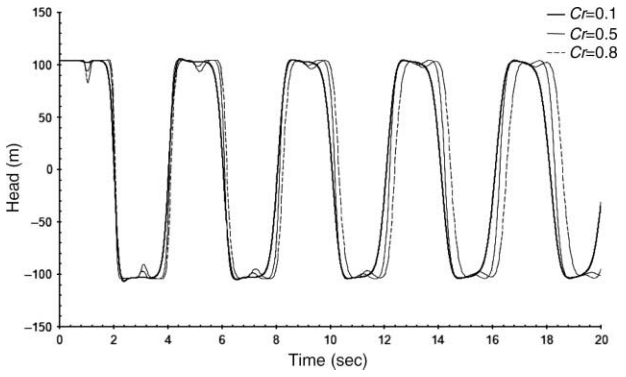

Figure 11 | Pressure head traces at valve position of a frictionless pipe computed by present FV solver for various Cr numbers.

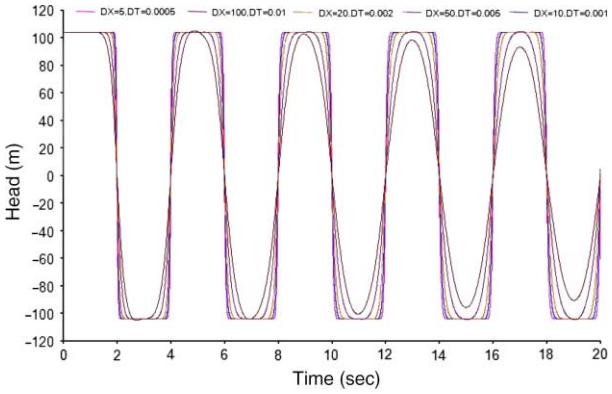

Figure 12 | Pressure head traces at valve position of a frictionless pipe computed by present FV solver for various mesh ($Cr = 0.1$).

The bend head loss coefficient may be calculated for certain angles as shown in Figure 8 and stored for in the computer for the use of computations. However, interpolation between the bend head loss coefficients for various angles would help calculating accurate coefficient for desired bend angle.

AUTOMATIC MODIFICATION OF STRESS DISTRIBUTION PIPELINE SEGMENTS

The maximum pressure distribution along the pipe line which is computed by the developed flow solver and the pipe specifications (D and t) as well as its material property ($\sigma_{\text{allowable}} = S.F \times \sigma_{\text{yield}}$) can be used for calculation of pipe

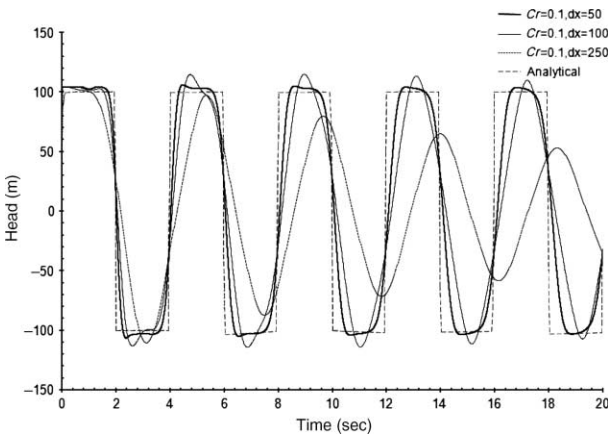

Figure 13 | Variations in Pressure head traces at valve position of a frictionless pipe computed by present FV solver for various mesh($Cr = 0.1$) with analytical solution.

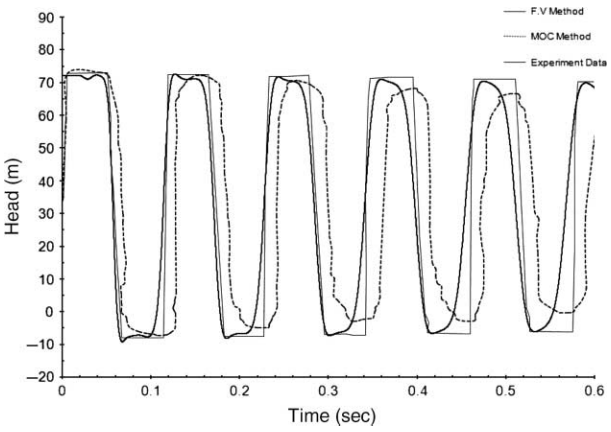

Figure 14 | Variations in hydraulic head at the valve position for a pipe with friction resulted from MOC and present FV solvers and compared with laboratory measurements.

thickness. Hence, using the maximum pressure values at segments of a pipe line system which are resulted from the developed model, distribution of maximum circumferential stresses along in the segments of the pipe line system can be computed using following relation,

$$\sigma = \frac{\rho g H \times D}{2t} \tag{30}$$

Long the pipe line system either the pipe segments geometric features (thicknesses or diameters) or their material properties can be modified via some iterative application of developed model for transient pressure pipe. Therefore, variable specification can be considered for a multi segments pipe line system.

For instance, the pipe thickness (t) of each segment can be modified by some trial iterations of the flow solver and using following relations.

$$t = \frac{\rho g H_{\max} D}{2\sigma_{\text{allowable}}} \tag{31}$$

Note that, the pressure distributions in pipe segments may vary as consequences of changing the pipe segments specifications, while, the pipe segments specifications should be modified as results of for a computed pressure distributions in pipe segments. Therefore, a trial iterative procedure is needed to achieve the uniform stress distribution along a multi segments pipe line system.

PRESSURE VERIFICATION RESULTS

In this section, the accuracy and efficiency of FV model (which is developed using Godunov scheme in solving transient continuity and equation of motion for water hammer problems) is assessed. First, the analytical solution results for a single frictionless pipe case are used for assessment of the *Cr*. Number on the accuracy of the results. Then, the computed results for a case with considerable pipe friction are compared with laboratory measurements.

Test case without friction

The first test case consists of a simple reservoir-pipe-valve configuration (Figure 9). The geometrical and hydraulic parameters for this frictionless test case are given in Table 1. This problem is solved by previous workers using a Godunov scheme for solving the continuity equation and momentum equation in which the convective term is omitted (Zhao & Ghidaoui 2004).

MOC results (Zhao & Ghidaoui 2004) as well as analytical solution are used to investigate the accuracy of proposed model which uses Godunov scheme for FV solution of the continuity equation coupled with momentum equation, which includes the convective term.

Figure 10 shows the comparison of the results computed by present FV method with analytical solutions and results of the MOC for the variations in hydraulic head at the valve as a function of time. As expected, the head traces results by both schemes (MOC and FV) exhibit numerical dissipation for $Cr = 0.1$, but the numerical dissipation in FV is considerably less than the MOC. It worth noting that, the finite volume solution using Godunov scheme corresponds to the analytical solution when $Cr = 1.0$. But for Courant

Table 3 | Initial properties for application of the developed model for automatic modification

Yield stress (N/m^2)	Unsteady friction coefficient	Mod. Of elasticity (kg/m^2)	Diameter (m)	Darcy factor
$2{,}400 \times 10^5$	0.015	2.07×10^{11}	2.6	0.015

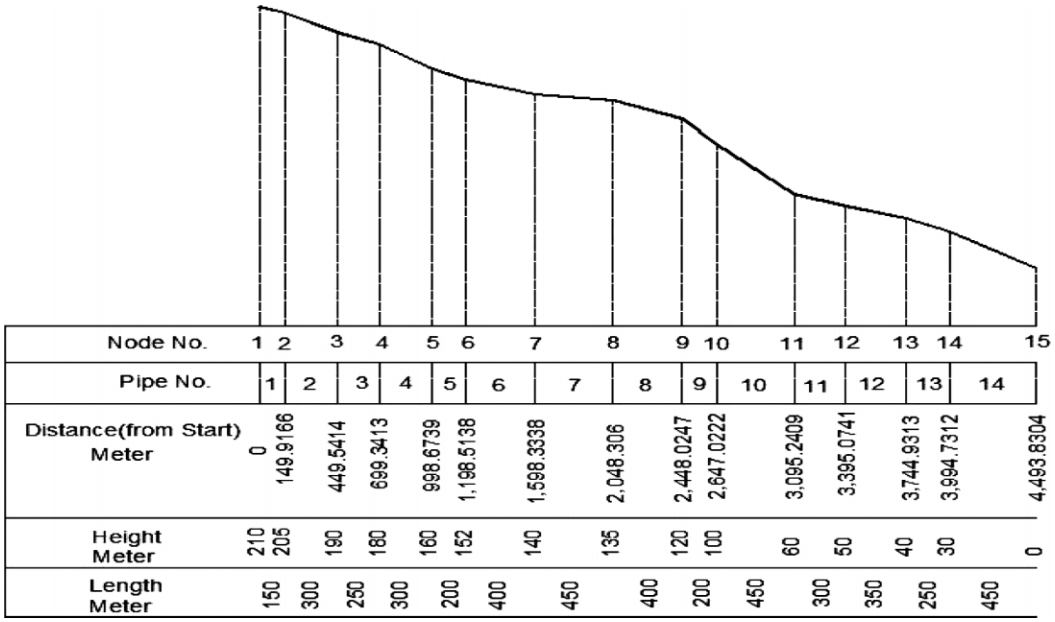

Figure 15 | A serial pipe line system with variable segments specifications considered for application of the developed model for automatic stress modification.

numbers less than one, the minor numerical dissipations appear in the FV solution results (Figures 11, 12 and 13).

Test case with friction

For the second test case, laboratory data (Bergant & Simpson 1994) for a closure of a valve downstream in 0.009 seconds of a pipe with wall roughness are used to investigate the accuracy of present FV method. The geometric, kinematics, and dynamic parameters of this test are summarized in Table 2.

In Figure 14 the results of present FV and MOC solvers (Bergant & Simpson 1994) are compared with laboratory measurements. As can be seen in Figure 14, although the time period of the pressure waves are computed reasonably by both numerical models, present FV solver produce much better distribution of the pressure values than the MOC.

APPLICATION OF THE MODEL FOR STRESS MODIFICATION

In order to present the ability of the developed model to deal with variation of the pipe characteristics (i.e. segment lengths, coordinates, slopes and thicknesses) is assessed. In this section, the developed model is applied for automatic modification of the pipe segments specification in a serial pipe line system which is presented in Figure 15. The details of initial assumption for the pipe line system are tabulated in Table 3.

Considering sudden closure of the downstream valve of the pipe line system, assumed uniform conditions for the geometrical features and material properties along the pipe line would result non-uniform stress distribution in the segments of the pipe line. After some automatic trial iterations, conservative uniform distribution of the maximum and minimum working stresses along the pipe line segments is achieved (Figures 16 and 17).

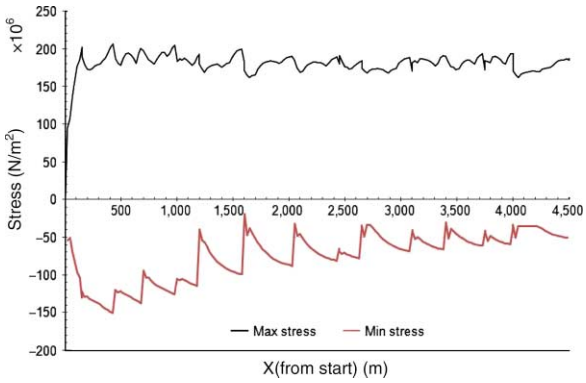

Figure 16 | Relatively uniform distribution of maximum and minimum stresses along a pipeline resulted from automatic modifications ($\sigma = \rho gHD/2t$).

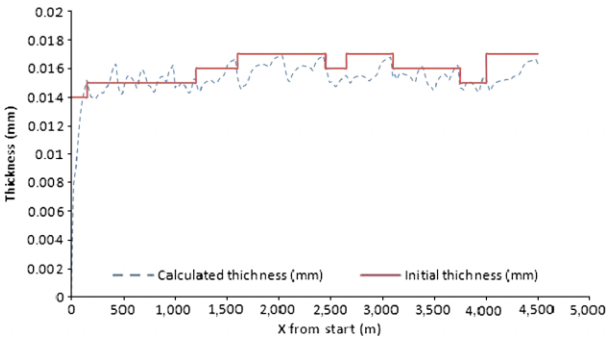

Figure 17 | Comparison between initial thickness (at first) and calculated thickness along a pipeline resulted from automatic modifications.

CONCLUSION

In this article, firstly, the accuracy and efficiency of a second-order Godunov-type FV model for coupled solution of transient velocity and pressure fields are investigated. The numerical model solves continuity equation and momentum equation (with convective term) in a coupled manner. The results of present FV solver are compared with numerical data produced by a MOC model, analytical solution as well as measured data reported by other researchers for frictionless and rough pipes, respectively. Finally, the computational tool is developed for automatic modification of the pipe line segment specifications.

The conclusions on the results of present numerical investigations are as follows:

- The nonlinear convective terms to the mathematical equations do not disturb the solutions to the water hammer problems.
- The present Godunov-type FV solver can be used for the water hammer problems in which the convection effect is not negligible (i.e. transient flow in pipes with large sections).
- The characteristics of pressure waves for transient flow in frictionless and frictional pipes computed by present FV solver are in close agreements with analytical and experimental data.
- For the Godunov-type FV flow solver part of the model, numerical dissipation is less than MOC, and therefore, the FV solver provides more accuracy than the MOC for certain Courant numbers less than one.
- The developed model is able to use the maximum computed pressure distribution along the pipeline with variable specifications (i.e. segment lengths, coordinates, slopes and thicknesses) to automatically modify the pipe segments thicknesses, in such a way that uniform stress distribution results all over the pipe segments.

ACKNOWLEDGEMENTS

The technical information supplied by Water & Energy Co. is greatly acknowledged.

REFERENCES

Abbasi, A. & Sabbagh-Yazdi, S. R. 2009 Upwind finite volume solution of water hammer in pipes without column separation using unsteady friction model. *Iran. J. Hydraulic* (in press), (Farsi).

Afshar, M. H. & Rohani, M. 2008 Waterhammer simulation by implicit method of characteristic. *Int. J. Pressure Vessels Piping* **85**, 851–859.

Balino, J. L., Larreteguy, A. E., Lorenzo, A. C., Padilla, A. G. & Lima, F. R. A. 2001 The differential perturbative method applied to the sensitivity analysis for waterhammer problems in hydraulic networks. *Appl. Math. Model.* **25**, 1117–1138.

Bergant, A. & Simpson, A. R. 1994 Estimating unsteady friction in transient cavitating pipe flow. *Proceeding of Second International Conference on Water Pipe Line Systems*, Edinburgh, UK, 24–26 May 1994, Conf. Series Publ. 110, 3–15.

Chaudhary, M. H. & Housaini, M. Y. 1985 Second order accurate explicit finite difference schemes for waterhammer analysis. *J. Fluids Eng.* **107**, 523–529.

Ghidaoui, M. S. & Karney, B. W. 1994 Equivalent differential equations in fixed-grid characteristics methods. *J. Hydraulic Eng.* **120**(10), 1159–1175.

Guinot, V. 2000 Riemann solvers for water–hammer simulations by Godunov method. *Int. J. Numer. Meth. Eng.* **49**, 851–870.

Jovic, V. 1995 Finite element and method of characteristics applied to water hammer modeling. *Int. J. Eng. Model.* **4**(3–4), 21–28.

Pezzinga, G. 2000 Evaluation of unsteady flow resistance by Quasi-2D or 1D models. *J. Hydraulic Eng.* **126**(10), 778–785.

Zhao, M. & Ghidaoui, M. S. 2004 Godunov-type solution for waterhammer flows. *J. Hydraulic Eng.* **130**(4), 341–348.